Research Article | Vol. 28, No. 14 / 6 July 2020 / Optics Express 21300
Optics EXPRESS

Individual inscription of spectrally multiplexed Bragg gratings in optical multicore fibers using small spot direct UV writing

SENTA L. JANTZEN,[1,*] REX H. S. BANNERMAN,[1] ALEXANDER JANTZEN,[1] PAOLO L. MENNEA,[1] DEVIN H. SMITH,[1] JAMES C. GATES,[1] LEWIS J. BOYD,[2] PETER G. R. SMITH,[1] AND CHRISTOPHER HOLMES[1]

[1] *University of Southampton, Southampton, UK*
[2] *Parker Aerospace, Parker Hannifin Corporation, Bristol, UK*
[*] *s.jantzen@soton.ac.uk*

Abstract: We have demonstrated the inscription of Bragg gratings into five individual cores of a seven core fiber using small spot direct UV writing. With this technique, we defined spectrally multiplexed Bragg gratings consecutively in separate cores as well as spectrally multiplexed gratings at the same longitudinal location in different cores. The effect of bending on the optical spectrum was evaluated to allow the differentiation between cross-exposure and cross-talk, and an alignment process to reduce cross-exposure by 13 dB was found.

1. Introduction

Fiber Bragg gratings (FBGs) are periodic refractive index patterns inscribed longitudinally in the core of an optical fiber. These refractive structures cause light of a certain wavelength to constructively interfere and create a characteristic spectral response in transmission and reflection. These gratings are often used for sensing and filtering as their spectral response is sensitive to strain and thermal variations and can be engineered for a specific wavelength, grating reflectivity and grating apodization [1–3]. This flexibility makes FBGs ideal filters and sensors for various applications, for example for emission line filtering in astronomy [4,5], vibration monitoring for structural architectures [6] and temperature monitoring in harsh environments [7].

High thermal stability, chemical inertness, and immunity to electromagnetic interference are key attributes for using FBGs in harsh environments, while their sensitivity to temperature and strain allows them to be deployed as sensors and particularly as bend and shape sensors [3,8,9]. Temperature and strain, however, both vary the nominal wavelength of the Bragg grating, which makes it difficult to separate those effects from each other.

Recent developments in fiber fabrication offer a solution to separate temperature, bending strain and fiber twist from each other: the development of multicore fiber with a central core. With the central core being in the neutral axis, a Bragg grating in this central core will only experience thermal and longitudinal strain effects, which allows thermal and longitudinal strain referencing for other gratings. The gratings in outer cores of a multicore fiber experience different amounts of strain depending on their position relative to the bending plane and from twist along the fiber. This enables the Bragg gratings to measure strain in the fiber due to bend, twist and thermal variation, allowing this device to be used for shape sensing.

Different techniques that have been used to inscribe Bragg gratings into multicore fiber are schematically illustrated in Fig. 1. Flockhart et al. reported the first inscription of FBGs into three of a four-core hydrogenated fiber using a phase mask [6]. In that work all cores were exposed

#396798 https://doi.org/10.1364/OE.396798
Journal © 2020 Received 5 May 2020; revised 11 Jun 2020; accepted 14 Jun 2020; published 2 Jul 2020

Optics EXPRESS

with one mask, resulting in the same grating inscription in three cores. However, due to the different location of the cores, the alignment was not ideal for all cores resulting in a significant variation of the grating spectra. Barrera et al. used a uniform phase mask and translated the mask relative to the fiber movement to achieve apodized gratings with comparable spectra in four cores of a hydrogenated four-core fiber [10]. In an alternative approach, Lindley et al. used a flat top capillary to provide uniform exposure and therefore uniform grating properties across all seven cores of their fiber, again with a phase mask [5].

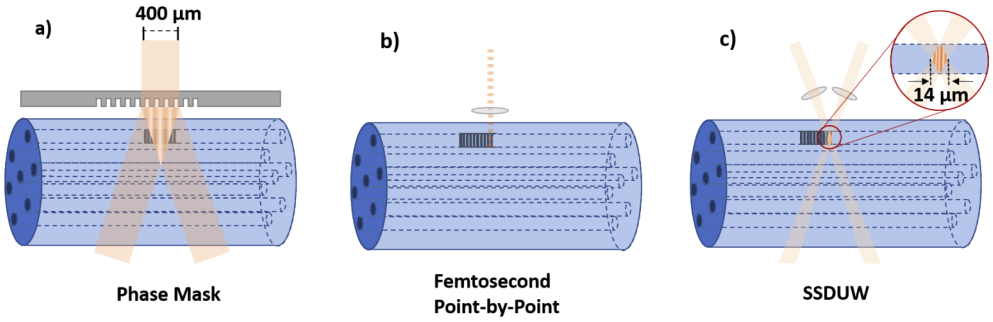

Fig. 1. Schematic overview of different writing techniques for multicore fiber: a) phase mask inscription, b) femtosecond point-by-point writing c) small spot direct UV writing (SSDUW).

Phase mask writing is commercially used to fabricate cost-efficient Bragg gratings; the drawback for using phase masks in multicore writing is the limitation in core selectivity. This technique exposes all cores simultaneously, but does not allow the inscription of gratings at different wavelengths into different cores, at the same physical location. In order to minimize interrogation equipment and so reduce cost, it is beneficial for certain applications to combine all cores for interrogation and use only one interrogator system. To analyze the grating spectra of all cores in one channel, spectral multiplexing is required, otherwise gratings of different cores would spectrally overlap. This approach is difficult to realize using a phase mask.

A different writing technique, femtosecond point-by-point writing, enables selective writing into individual cores of a multicore fiber by focusing a femtosecond laser into individual cores. This technique does not require hydrogenation of the fiber. Donko et al. demonstrated the grating inscription of four cores of a seven-core fiber in a wavelength range between 1532-1548 nm [11]. Wolf et al. reported the inscription of gratings into four cores of a seven-core fiber, all located at the same longitudinal position [12]. Femtosecond point-by-point writing techniques allow inscription into individual cores, however, the gratings reported are Type II-IR, which are attributed to micro-voids in the material structure. This typically introduces significantly higher scattering losses compared to phase mask written gratings [13]. In FBG sensing applications it is desirable to have multiple FBGs in the sensor, as this enables more sensing points, which can lead to higher sensing accuracy and spatial resolution. High losses caused by FBG inscription are therefore to be avoided where possible.

The small spot direct ultraviolet writing (SSDUW) technique can be considered as an in-between of the two techniques previously explored in Figs. 1 (a) and (b) as it combines UV inscription typically used in phase mask fabrication with a small, focused beam. The spot size is comparable to the width of the cores, such that the exposure can be focused in individual cores [7]. In this paper, we demonstrate a novel technique for the inscription of spectrally multiplexed Bragg gratings into individual cores of a seven-core fiber. This technique allows cost-effective inline monitoring and provides more data points per location. We evaluated the effect of bending

Optics EXPRESS

on the optical spectrum to differentiate between cross-exposure and cross-talk and analyzed an alignment process to reduce cross-exposure by 13 dB.

2. Fabrication and results

The multicore fiber used here was provided by Fibrecore Ltd. It is a seven core fiber with a core spacing of 34.5 μm. The Germanium doped cores are arranged in a hexagon shape with one core in the center. This fiber was hydrogen loaded for 14 days at 120 bar and room temperature prior to writing, to enhance UV photosensitivity. The polymer coating was removed, and both ends of the fiber clamped into rotatable fiber holders with a tension of 0.5 N to straighten the fiber.

The FBGs were fabricated using the SSDUW technique, shown in Fig. 2, where fiber clamps installed on nanometer-precision Aerotech air-bearing stages translate a fiber underneath an interference laser spot. The translation velocity of the fiber defines the fluence that is introduced into the core. The inscription time of a grating is dependent on the fluence which is proportional to the laser output power. With an average power of 27 mW, it takes approximately 4 minutes to inscribe a 7 mm grating. A beam of a 244 nm frequency-doubled argon-ion laser light is divided into two arms before being focused and combined into a 14 μm diameter interference spot in one core of the fiber. This interference spot completely covers the 5 μm diameter fibre core of the multicore fibre. The fixed crossing angle defines the interference pattern spacing and therefore the central Bragg wavelength, which is designed to be 1550 nm. An electro-optic modulator (EOM) driven with a sawtooth signal is introduced into one of the interferometer arms, which allows the fringes to be synchronized with the movement of the fiber. The spatial period of the sawtooth wave defines the Bragg period, allowing for wavelength detuning.

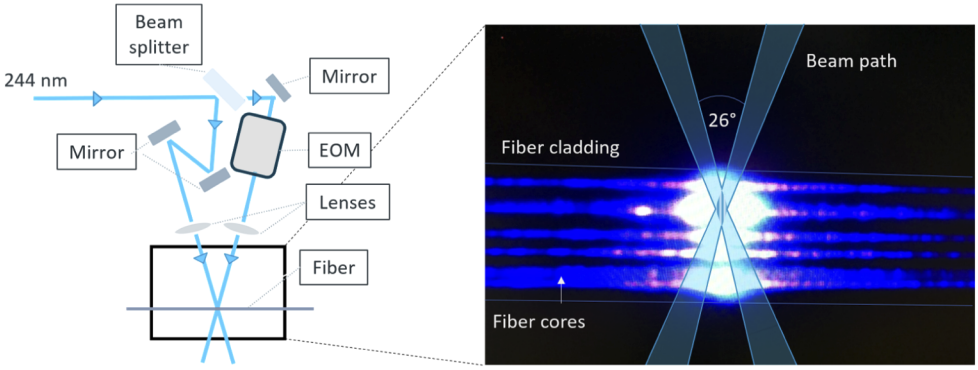

Fig. 2. Small spot direct UV writing set up on the left with an insert of the multicore fiber during writing. Two beams of a 244 nm frequency-doubled argon-ion laser are focused into one core of a multicore fiber, where they interfere and create an interference pattern. This pattern defines the Bragg grating.

With the small size of the interference spot we aim to only structure a single core of a multicore fiber without exposing neighboring cores; furthermore, approximately 26 gratings planes are exposed at once, which allows fabrication of gratings with almost arbitrary apodization profiles. As shown in Fig. 2, the UV induced photoluminescence illuminates all seven cores in the fiber, but focused primarily into only a single core. The crossing point of the two laser beams was aligned into one core by moving the fiber vertically and adapting its horizontal position.

A set of six 7 mm long gratings were inscribed into five different cores at consecutive positions as shown in Fig. 3 (a). We initially moved the fiber laterally and vertically to identify the position of the cores using the fluorescence of the cores at illumination with the laser. Once the core was identified, we started with the grating inscription. This means that the exposure of other

Optics EXPRESS

cores was initially uncontrolled; however, this method has been improved as later discussed. Due to limitations in the stability of the Argon laser and hydrogen out-diffusion all the writing was carried out within a 4-hour window, which limited us to inscribe five cores in this device. Table 1 shows the design Bragg period for the gratings in Fig. 3.

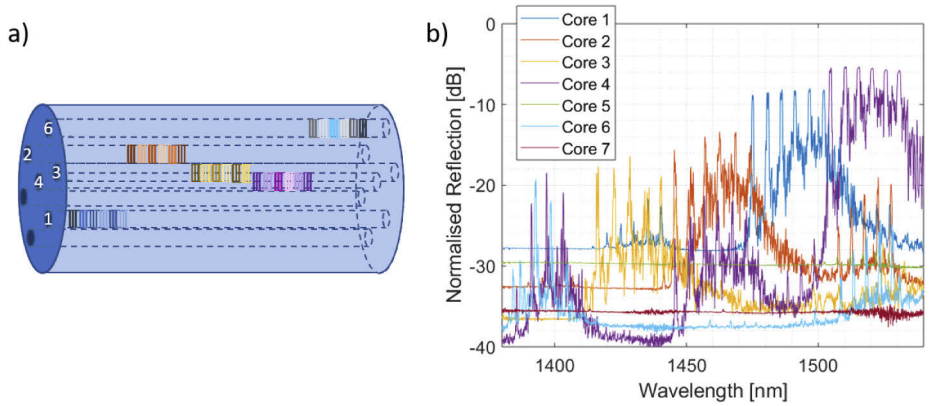

Fig. 3. a) Schematic of grating location in the multicore fiber and b) resulting optical reflection spectrum of each core. Each colour in b) represents the optical spectrum of one core. The colour in a) matches to the spectrum in b). The optical spectra are overlaid to demonstrate spectral cross-exposure between cores.

Table 1. Design period for Bragg gratings shown in Fig. 3

	Grating Period [nm]				
	Core 1	Core 2	Core 3	Core 4	Core 6
Grating 1	507.8	497.5	487.2	518.0	476.9
Grating 2	509.5	499.2	488.9	519.8	478.6
Grating 3	511.2	500.9	490.6	521.5	480.3
Grating 4	512.9	502.6	492.3	523.2	482.0
Grating 5	514.6	504.3	494.0	524.9	483.7
Grating 6	516.3	506.0	495.7	526.6	485.5

For interrogation, a broadband super luminescent light source (Amonics ASLD-CWDM-5B-FA) was connected to an optical spectrum analyzer via a 3 dB coupler. A fan-out was used to individually interrogate the multiple cores. The corresponding optical reflection spectrum is shown in Fig. 3 (b). A concern of this presented optical spectrum is the appearance of grating spectra in cores, where these spectra were supposedly not inscribed. So appears core # 4 for example to have three sets of Bragg gratings inscribed: one set around 1400 nm, one set around 1460 nm and one set around 1520 nm. Only the set around 1520 nm was intentionally inscribed into this core. Evidence of this effect can be seen later in Fig. 4.

There are two effects that can cause such spectral artifacts: cross-talk and cross-exposure. Cross-talk could be caused by the fan-out and appears when imperfect core alignment at the fan-out/multicore fiber interfaces allows light to couple from one core into another. The output is then a combination of multiple cores, which causes FBGs of one core to appear in the optical spectrum of a different core. Cross-exposure on the other hand appears when cores are unintentionally exposed during the writing process. These two effects may be separated through bend testing. Bending the multicore fiber induces different amounts of strain in the cores, depending on their location relative to the bending plane. This variation in strain will cause the

Optics EXPRESS

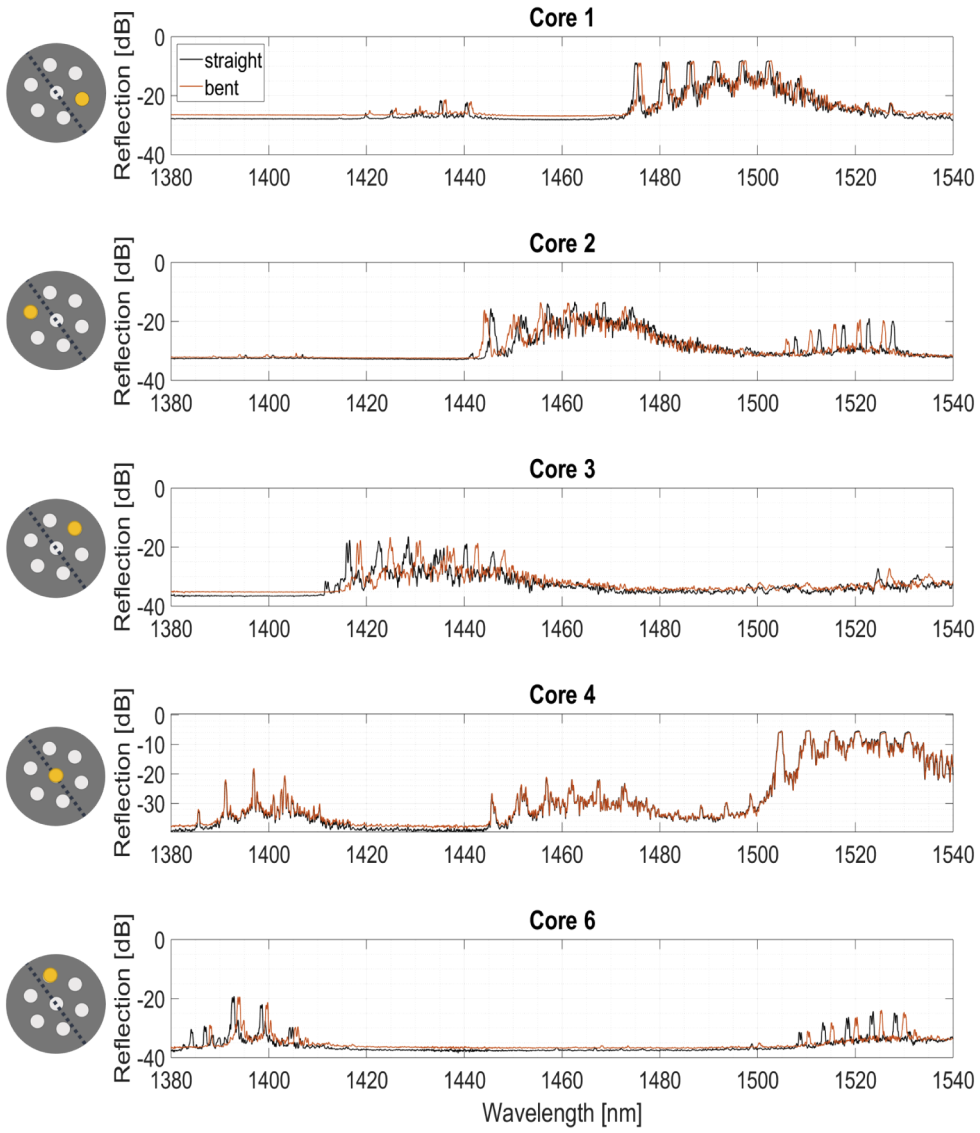

Fig. 4. Strain, for example due to bending shifts the optical response of a Bragg grating. This spectral response can be used to determine the location of the core relative to the bending plane. The schematic on the center indicates the core position relative to the bending plane represented by a dotted line. The central core, core #4, shows no shift due to bending, as this lies on the neutral axis.

Optics EXPRESS

spectral response of the FBGs to shift according to the amount of strain. If the optical response of all FBGs in one core shift by approximately the same amount, it can be assumed that these FBGs are inscribed into this one core. In this case, the spectral artifacts are due to cross-exposure. If however not all FBGs shift by approximately the same amount, it can be assumed that light coupled between the cores. This would then suggest that the underlying effect for such spectral artifacts is cross-talk. In the following section, the bending response is analyzed to evaluate the origin of the spectral artifacts and thus assess the inscription technique.

2.1. Bending response

To evaluate the origin of the previously mentioned spectral features and with it, to analyze the quality of the inscription technique, the fiber was exposed to bending. The spectral response of the grating subject to bending is shown in Fig. 4. The fiber was wrapped around a cylinder with a diameter of 25.4 ± 0.5 mm. Evaluating the spectral response of FBGs during bending not only clarifies the nature of the spectral artifacts and if they are a result of cross-talk or cross-exposure, but it can also identify the relative locations of the cores with respect to the bending plane. Compressing a Bragg grating will induce a blue shift, whereas tensioning will result in a red shift. The location of the Bragg gratings within the multicore fiber are schematically shown on the left in Fig. 4.

Evaluating the optical spectrum of each core in Fig. 4 on its own, allows to concluded that the spectral artifacts are a result of cross-exposure, since all grating features (including artifacts) in each individual core shift by comparable amounts. Note this response is most notable in the central core, which being on the neutral axis experiences no shift. This undesired cross-exposure can be seen as a drawback of the inscription technique, however, it has been found to be caused by an inefficient alignment process. This will be further discussed in the following section.

As indicated in Fig. 4, the spectral shift due to bending varies between the cores depending on their position relative to the bending plane. For example, the spectral peak for the FBG in core #3 shifts by 2.3 nm, in core #6 by 1.3 nm and in the central core, core #4, by 0.08 nm. This small shift is due to unavoidable strain from winding tension and temperature variation. As the core lies on the neutral axis and therefore does not experience strain due to twist or bend, the shift in the central core was subtracted from the outer cores as a reference. The axial strain ε_1 for core #n is [1]

$$\varepsilon_n = 0.78\,\frac{\Delta\lambda_{Bn}}{\lambda_{Bn}}, \tag{1}$$

with the strain optic correction factor of 0.78 in silica fiber, the spectral shift in Bragg wavelength in core #1 $\Delta\lambda_{B1}$ and the central Bragg wavelength in core #1 λ_{B1}. The axial strain of the other outer cores is calculated respectively.

Thermal variation, bending and axial strain are not the only effects causing a shift in the optical spectrum of an FBG. The fiber may also experience twist, which is effectively equivalent to an axial strain for all outer cores. The strain for each core is

$$\begin{pmatrix} \varepsilon_1 \\ \varepsilon_2 \\ \varepsilon_3 \\ \varepsilon_4 \\ \varepsilon_6 \end{pmatrix} = \begin{bmatrix} 1 & A_1 & B & \alpha \\ 1 & A_2 & B & \alpha \\ 1 & A_3 & B & \alpha \\ 1 & 0 & 0 & \alpha \\ 1 & A_6 & B & \alpha \end{bmatrix} \begin{pmatrix} \varepsilon_{\text{axial}} \\ r^{-1} \\ \Omega \\ \Delta T \end{pmatrix}, \tag{2}$$

where the strain experienced for each respective core, ε_i, is the sum of several components: The axial strain $\varepsilon_{\text{axial}}$ and the thermal fluctuations $\alpha\Delta T$ are assumed to be equal for all cores, where α

Optics EXPRESS

is the thermal expansion coefficient; the strain induced by bending forms the second coefficient $A_i r^{-1}$, where A relates to the function outlined in Fig. 5; the third component refers to the strain induced by twist, where B depends upon the distance that the cores are set away from the center and Ω is the twist per unit length. The twisting strain is approximately equal for all cores except the central core (# 4), which we assume to be negligible.

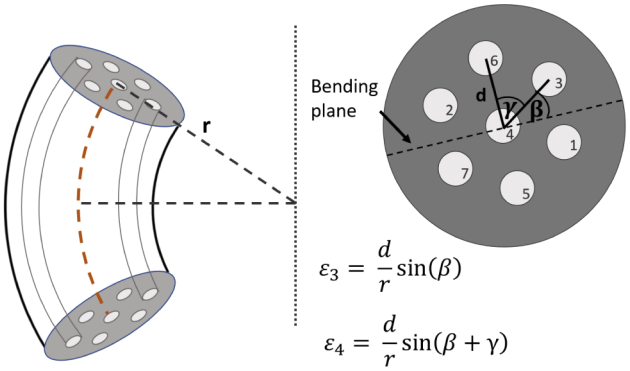

Fig. 5. A multicore fiber bent at radius r with cross-section shown upper right. Axial strain ε_i experienced in each core is related to its distance from the neutral axis.

Using Eqs. (2) and the measured values of ε via Eq. (1), we are able to derive the bend radius r. The core separation of the multicore fiber is 34.5 μm, each core is 5 μm in diameter and the fiber diameter measures 125 μm. With ε, the equation in Fig. 5 and the set of equations in Eqs. (2), there are five unknowns (β, r, A_n, Ω, ΔT) and five equations. The diameter of the cylinder (measured diameter = 25.4± 0.5 mm) was calculated to be 27 ± 2 mm. The fiber manufacturer states an error of approximately 1% on the cladding diameter of the fiber and it was assumed that all dimensions vary by approximately this amount [14].

2.2. Reduced cross-exposure inscription

The large amount of cross-exposure in the reflection spectrum in Fig. 3 (b) is desired to be minimized. In an attempt to reduce the cross-exposure of the technique, the alignment process was altered such that instead of just linearly translating the focus of the dual beams, the fiber was also rotated about its axis (like the barrel of a revolving pistol) to ensure that the targeted core is the upper most and closest to the UV beams. This method was to align and inscribe the central core first and then rotate the fiber about its axis until the crossing of the laser beams target the next core. This can be identified by monitoring the fluorescence of the cores with a camera. For fine alignment, the fiber was then again vertically and laterally translated to ensure the cross section to be aligned in the desired core. This allows the two beams to be focused directly in the desired core and reduces diffraction due to neighboring cores.

To demonstrate this approach, the inscribed FBGs were spatially multiplexed as shown in Fig. 6 (a). This consists of two Gaussian apodized Bragg gratings (each 7 mm long) with a spectral spacing of 5 nm, written into four individual cores. All gratings were spectrally multiplexed. The first two sets were defined in different cores at the same longitudinal location, whereas the following two sets were written sequentially into different cores. The spectral response of the individual cores is shown in Fig. 6 (b).

This fiber shows significantly less cross-exposure; reducing from 1.7 dB between core #2 and #4 in Fig. 3 (b) to 14.7 dB between core #1 and #4 in Fig. 6 (b), assuming equal coupling efficiency between cores. These values were determined by subtracting the peak amplitudes at 1462 nm between core #2 and core #4 in Fig. 3 (b) and at 1464 nm between core #1 and core #4 in

Optics EXPRESS

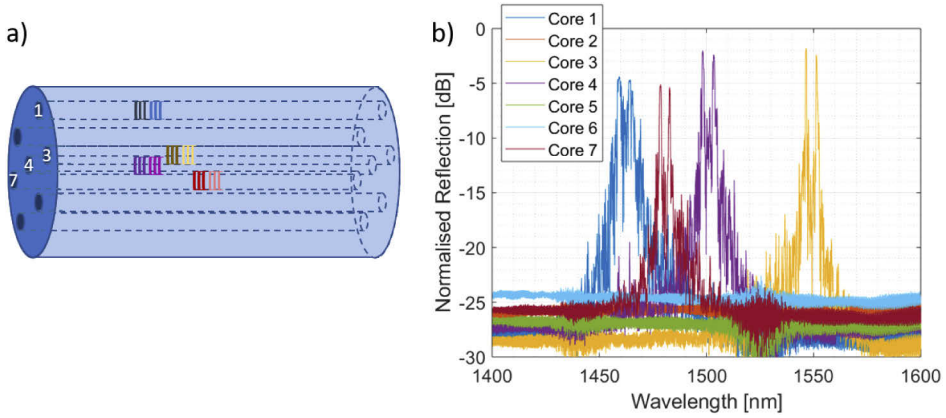

Fig. 6. Two Bragg gratings inscribed into each core. a) Schematic overview of the grating location. b) Optical reflection spectrum of all cores overlaid. The grating color in b) corresponds to the grating location in a).

Fig. 6 (b) after normalizing the background reflection. Individual plots of the gratings are shown later in Fig. 7. The desired decrease in cross-exposure can be ascribed to a more consistent alignment process, where the targeted core was aligned to be the uppermost core. The crossing point of the two incoming laser beams was therefore directly focused in this core, without being diffracted by neighboring cores. This fiber alignment was achieved by rotating the fiber like the barrel of a revolver. This shows that SSDUW is capable of defining gratings at the same longitudinal location in different cores of a multicore fiber with negligible cross-exposure.

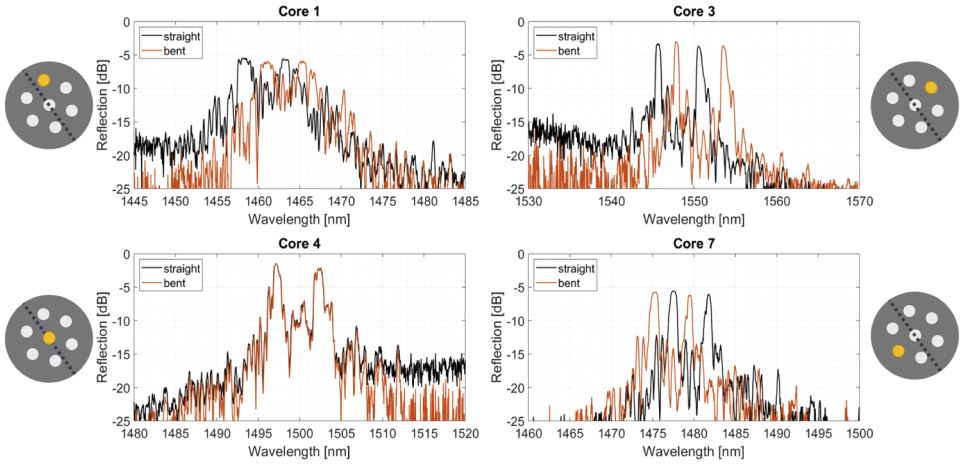

Fig. 7. The relative shift of the optical reflection spectrum was used to determine the position of the cores in the multicore fiber. The schematics on the right and left visualise the location of the cores relative to the bending plane.

The spectrum along with the location of the cores relative to the bending plane is shown in Fig. 7. The central core #4 displays no spectral shift in response to bending. Gratings inscribed into cores on opposite bending planes (core #3 and #7) show an opposing spectral shift. Bending was again used to identify the location of the cores, particularly the central core.

Optics EXPRESS

3. Conclusion

We demonstrate for the first time the inscription of fiber Bragg gratings into selective cores of a multicore optical fiber using small spot direct UV writing. We demonstrated the inscription of gratings at the same longitudinal position along the fiber, but in different cores.

To establish the location of the cores in the multicore fiber, an optical reflection spectrum of the bent fiber was taken and compared to the optical reflection spectrum of the straight fiber. This allowed to determine the core location relative to the bending plane and to identify the central core.

We reduced undesired cross-exposure by 13 dB by addressing the cores through rotation during the alignment process. With this alignment process, we assured that the desired core is uppermost, which reduces undesired exposure and diffraction on neighboring cores. We also introduced bending as a technique to distinguish cross-exposure from cross-talk.

This work presents a novel method for individual inscription into selected cores of a multicore fiber. It allows to fabricate more sensing points in a single location by co-locating the gratings on the same longitudinal location in different cores offering future enhanced sensing capability.

Funding

Engineering and Physical Sciences Research Council (EP/K034480/1, EP/M013243/1, EP/M013294/1, EP/M024539/1, EP/M508147/1); Parker Aerospace, Parker Hannifin Corporation.

Acknowledgments

We would like to thank Fibercore Ltd for providing the multicore fiber to conduct this research. Further, we would like to thank Ali Masoudi and Angeliki Zafeiropoulou for their valuable collaboration.

Disclosures

SLJ: Parker Aerospace, Parker Hannifin Corporation (F), LJB: Parker Aerospace, Parker Hannifin Corporation (E).

Data Availability

Data published in this paper are available from the University of Southampton repository at https://doi.org/10.5258/SOTON/D1416.

References

1. R. Kashyap, *Fiber Bragg Gratings* (Elsevier Inc., 2010).
2. M. Amanzadeh, S. M. Aminossadati, M. S. Kizil, and A. D. Rakić, "Recent developments in fibre optic shape sensing," Meas. J. Int. Meas. Confed. **128**, 119–137 (2018).
3. O. V. Butov, A. P. Bazakutsa, Y. K. Chamorovskiy, A. N. Fedorov, and I. A. Shevtsov, "All-fiber highly sensitive bragg grating bend sensor," Sensors **19**(19), 4228 (2019).
4. T. A. Goebel, M. Weissflog, R. G. Krämer, M. Heck, D. Richter, and S. Nolte, "Tuning multichannel filters based on FBG in multicore fibers," Proc. SPIE **10908**, 1090800 (2019).
5. E. Lindley, S.-S. Min, S. Leon-Saval, N. Cvetojevic, J. Lawrence, S. Ellis, and J. Bland-Hawthorn, "Demonstration of uniform multicore fiber Bragg gratings," Opt. Express **22**(25), 31575 (2014).
6. G. M. H. Flockhart, W. N. MacPherson, J. S. Barton, J. D. C. Jones, L. Zhang, and I. Bennion, "Two-axis bend measurement with Bragg gratings in multicore optical fiber," Opt. Lett. **28**(6), 387 (2003).
7. S. L. Scholl, A. Jantzen, R. H. S. Bannerman, P. C. Gow, D. H. Smith, J. C. Gates, L. J. Boyd, P. G. R. Smith, and C. Holmes, "Thermal approach to classifying sequentially written fiber Bragg gratings," Opt. Lett. **44**(3), 703–706 (2019).
8. R. Di Sante, "Fibre Optic Sensors for Structural Health Monitoring of Aircraft Composite Structures: Recent Advances and Applications," Sensors **15**(8), 18666–18713 (2015).

Optics EXPRESS

9. C. Holmes, S. Ambran, P. Cooper, A. Webb, J. C. Gates, C. B. E. Gawith, J. Sahu, and P. G. R. Smith, "Bend monitoring and refractive index sensing using flat fibre and multicore Bragg gratings," Meas. Sci. Technol. **31**(8), 085203 (2020).
10. D. Barrera, I. Gasulla, and S. Sales, "Multipoint Two-Dimensional Curvature Optical Fiber Sensor Based on a Nontwisted Homogeneous Four-Core Fiber," J. Lightwave Technol. **33**(12), 2445–2450 (2015).
11. A. Donko, M. Beresna, Y. Jung, J. Hayes, D. Richardson, and G. Brambilla, "Point-by-point inscription of Bragg gratings in a multicore fibre," *CLEO-Pacific Rim* pp. 2–3 (2017).
12. A. Wolf, K. Bronnikov, A. Dostovalov, and S. Babin, "Femtosecond pulse inscription of 3D arrays of Bragg gratings in selected cores of a multicore optical fiber," *CLEO/Europe-EQEC* **1170**, 630090 (2019).
13. R. J. Williams, R. G. Krämer, S. Nolte, and M. J. Withford, "Femtosecond direct-writing of low-loss fiber Bragg gratings using a continuous core-scanning technique," Opt. Lett. **38**(11), 1918–1920 (2013).
14. Multicore fiber,", https://www.fibercore.com/product/multicore-fiber (accessed 10 June 2020).